Occurrence of Intersubband Polaronic Repellons in a Two-Dimensional Electron Gas

Stefan Butscher* and Andreas Knorr

Institute for Theoretical Physics, Nonlinear Optics and Quantum Electronics, Technical University Berlin, PN 7-1 Hardenbergstraße 36, 10623 Berlin, Germany

(Received 13 January 2006; published 8 November 2006)

Counteracting electron-phonon and electron-electron interaction in the optical absorption spectra of a quantum well intersubband system can have a significant impact on the line shape and line width of optical transitions at low temperatures. In particular, polaronic repellons can be formed due to an attractive intersubband polaron-polaron interaction. At low temperatures and for properly chosen densities; this effect can lead to a line broadening of the intersubband transition, even in a weak coupling regime.

DOI: 10.1103/PhysRevLett.97.197401 PACS numbers: 78.67.De, 71.38.−k

Because of its ideal model character, intersubband (ISB) transitions in doped semiconductor quantum wells (QW) allow a significant insight into the many-particle physics of a two-dimensional electron gas [1]. Many-particle interactions in ISB transitions such as electron-electron (e-e) and electron-phonon (e-ph) interaction have been the subject of a series of theoretical investigations in a Green's function approach [2] and in the density matrix formalism [3,4].

In this Letter, we show that even for weak e-ph coupling, at properly chosen doping densities, attractive polaron-polaron (p-p) interaction counteracts the Coulomb repulsion and leads to a broadening of elementary ISB excitations. While it is well established that in a polar medium one observes a formation of polaronic excitons [5], for interband transitions, we introduce in analogy the term *polaronic repellon* for ISB transitions in a two-dimensional electron gas to describe this phenomenon.

Without the e-ph interaction, repellon resonances (as well as the exchange interaction and the depolarization shift) arise through the Hartree-Fock part of the Coulomb interaction between an electron optically transferred to the upper subband and the remaining electrons in the lower subband [6]. This is illustrated in a band structure diagram in Fig. 1. Beyond the mean-field approximation, second order correlation effects of the e-e and e-ph interaction introduce carrier scattering and optical dephasing. At room temperature, the line broadening due to these incoherent e-e and e-ph processes in the second Born-Markov approximation agree very well with experimental results [7,8]. Besides these incoherent processes, the e-ph interaction also changes the single-particle properties like energy and mass: Polaron formation takes place. Furthermore, two polarons have an attractive interaction between each other, besides the Coulomb repulsion. An excellent coverage of the polaron topic is given in Ref. [5]. So far, the p-p attraction has not been considered for ISB transitions. A fair sign that such effects, besides electron correlations, may be of importance for ISB transitions in a two-dimensional electron gas is seen from the fact that at lower temperatures, the agreement between theory and experiment is typically less good; for instance incoherent scattering process calculations underestimated the observed line width of ISB transitions [7,8]. Surely, better agreement can be achieved by including effects such as impurities [9] or interface scattering [10]. At low temperatures, however, a better understanding of the nature of the e-ph interaction—beyond incoherent scattering—is essential to understand high quality samples.

The Hamilton operators of the free phonons and electrons, the e-ph interaction, and the Coulomb e-e interaction are [11,12]

$$H_0 = \sum_{l\mathbf{k}} \varepsilon_{l\mathbf{k}} a^{l\dagger}_{\mathbf{k}} a^{l}_{\mathbf{k}} + \sum_{\mathbf{q}} \hbar\omega_{\mathrm{LO}} b^{\dagger}_{\mathbf{q}} b_{\mathbf{q}}, \tag{1}$$

$$H_{e\text{-ph}} = \sum_{l,m,\mathbf{k},\mathbf{q}} g^{lm}_{\mathbf{q}} a^{l\dagger}_{\mathbf{k}} a^{m}_{\mathbf{k}-\mathbf{q}_{\|}} b_{\mathbf{q}} + \mathrm{H.a.}, \tag{2}$$

$$H^{\mathrm{Coul}}_{e\text{-}e} = \frac{1}{2} \sum_{\mathbf{k}\mathbf{k}'\mathbf{p},lmno} V^{lmno}_{\mathbf{p}} a^{l\dagger}_{\mathbf{k}+\mathbf{p}} a^{m\dagger}_{\mathbf{k}'-\mathbf{p}} a^{n}_{\mathbf{k}'} a^{o}_{\mathbf{k}}. \tag{3}$$

Here, $a^{m\dagger}_{\mathbf{k}}$, $a^{m}_{\mathbf{k}}$ and $b^{\dagger}_{\mathbf{q}}$, $b_{\mathbf{q}}$ are creation and annihilation operators for electrons with wave vector $\mathbf{k}$ in subband m and for phonons with wave vector $\mathbf{q}$ ($\mathbf{q}_{\|}$ is its in-plane projection). With these operators, we can express ISB coherences $f^{12}_{\mathbf{k}} := \langle a^{1\dagger}_{\mathbf{k}} a^{2}_{\mathbf{k}} \rangle$, subband occupations $f^{ii}_{\mathbf{k}} := \langle a^{i\dagger}_{\mathbf{k}} a^{i}_{\mathbf{k}} \rangle$, and the phonon occupation number $n_{\mathbf{q}} = \langle b^{\dagger}_{\mathbf{q}} b_{\mathbf{q}} \rangle$. $g^{lm}_{\mathbf{q}}$ denotes the Fröhlich coupling matrix elements and $V^{lmno}_{\mathbf{p}}$ the Coulomb potential, with the two-dimensional wave vector $\mathbf{p}$.

In the following, we will discuss the origin of the repellon resonance in ISB subband systems (i) then we introduce a mean-field approach to discuss the polaron formation and p-p attraction (ii) and discuss the equations

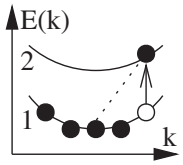

FIG. 1. Band structure of a two subband system in a QW. Optical ISB transition from subband 1 to subband 2. The dashed line illustrates the Coulomb interaction between electrons in different subbands.

of motion of the e-ph interaction (iii). Finally we present numerical results (iv).

(i)*Repellon resonances in ISB systems.*—In a doped semiconductor quantum well, the conduction subbands are thermally occupied with electrons. Thus, for typical ISB transitions (where due to band nonparabolicity the effective mass is larger in the upper subband) we have a repulsive Coulomb interaction of an electron optically transferred to the upper subband with an ionized electron continuum in the lower subband which leads to repellon formation, instead of the formation of excitons [13]. In order to form a stable eigenstate under such a repulsive interaction, every $\mathbf{k}$ state tries to transfer some of the oscillator strength to other momentum states. This is counterbalanced as long as these states are occupied. Hence, the oscillator strength is increased around the Fermi edge (repellon resonance) and decreased for all other states [6]. This mixing of different momentum states can also be seen in the Hartree-Fock semiconductor Bloch equations (HFB) [13]. The contribution responsible for the repellon formation in an ISB system reads

$$\dot{f}^{12}_{\mathbf{k}}|^{\mathrm{Coul}}_{e\text{-}e}|_{\mathrm{rep.}} = \frac{i}{\hbar}\sum_{\mathbf{p}\neq 0} V^{2121}_{\mathbf{p}}(f^{11}_{\mathbf{k}} - f^{22}_{\mathbf{k}})f^{12}_{\mathbf{k}+\mathbf{p}}. \tag{4}$$

Clearly, the ISB coherence at $\mathbf{k}$ is driven by the coherence at $\mathbf{k}+\mathbf{p}$. Note that the shift of the oscillator strength towards the Fermi edge can be shown by diagonalizing the HFB in the frequency domain.

(ii)*Multiband polaron approach.*—In the Heisenberg picture, we obtain the following equation of motion for a phonon annihilation operator $b_{\mathbf{q}}$:

$$\dot{b}_{\mathbf{q}} = -i\omega_{\mathrm{LO}} b_{\mathbf{q}} - \frac{i}{\hbar}\sum_{lm,\mathbf{k}} g^{lm*}_{\mathbf{q}} a^{m\dagger}_{\mathbf{k}-\mathbf{q}_\parallel} a^{l}_{\mathbf{k}}. \tag{5}$$

By applying a Markov approximation to this differential equation, we obtain an explicit solution of the inhomogeneous differential equation:

$$b_{\mathbf{q}} = \sum_{lm,\mathbf{k}} g^{lm*}_{\mathbf{q}} a^{m\dagger}_{\mathbf{k}+\mathbf{q}_\parallel} a^{l}_{\mathbf{k}}\left[\frac{\pi}{i}\delta(E^{ml+}_{\mathbf{k}+\mathbf{q}_\parallel,\mathbf{k}}) - \mathcal{P}(E^{ml+-\mathbf{1}}_{\mathbf{k}+\mathbf{q}_\parallel,\mathbf{k}})\right], \tag{6}$$

where we have introduced $E^{ml\pm}_{\mathbf{k}+\mathbf{q}_\parallel,\mathbf{k}} := \epsilon^{m}_{\mathbf{k}+\mathbf{q}_\parallel} - \epsilon^{l}_{\mathbf{k}} \pm \hbar\omega_{\mathrm{LO}}$. Here, we have neglected the homogeneous solution and thereby reduced the e-ph interaction to spontaneous emission of phonons, similar to the usual approach for photons [14]. This is valid for low temperatures with $n_{\mathbf{q}} \ll 1$. Later on, it turns out that only the principle value part $\mathcal{P}$ is responsible for the polaron formation and p-p attraction. Therefore, we replace $b_{\mathbf{q}}$ (and $b^{\dagger}_{\mathbf{q}}$) in Eq. (2) with the real part of Eq. (6) (and its adjoint). The resulting Hamilton operator can be divided into two components. The first one, containing two electronic operators, modifies the single-particle energies $\varepsilon_{l\mathbf{k}}$ (self-energy) and effective mass in the subband l. This is interpreted as polaron formation, the resulting Hamiltonian reads

$$H_{0,p} = \sum_{l\mathbf{k}}\left(\varepsilon_{l\mathbf{k}} - \sum_{\mathbf{q}_\parallel}\Lambda^{mlml}_{\mathbf{q}_\parallel,\mathbf{k}}\right)a^{l\dagger}_{\mathbf{k}} a^{l}_{\mathbf{k}}. \tag{7}$$

The remaining part of the Hamiltonian describes the p-p attraction and is given by

$$H^{p\text{-}p}_{\mathrm{ind}} = \frac{1}{2}\sum_{\mathbf{k}\mathbf{k}'\mathbf{q}_\parallel,lmno}\Lambda^{lmno}_{\mathbf{q}_\parallel,\mathbf{k}'} a^{l\dagger}_{\mathbf{k}+\mathbf{q}_\parallel} a^{m\dagger}_{\mathbf{k}'-\mathbf{q}_\parallel} a^{n}_{\mathbf{k}'} a^{o}_{\mathbf{k}},$$
$$\Lambda^{lmno}_{\mathbf{q}_\parallel,\mathbf{k}'} = \int \frac{g^{lo}_{\mathbf{q}} g^{nm*}_{\mathbf{q}}}{\pi}\mathcal{P}\left(\frac{1}{E^{mn-}_{\mathbf{k}'-\mathbf{q}_\parallel,\mathbf{k}'}} - \frac{1}{E^{mn+}_{\mathbf{k}'-\mathbf{q}_\parallel,\mathbf{k}'}}\right)d_{q_\perp}. \tag{8}$$

The p-p Hamiltonian Eq. (8) has a similar form as the Coulomb Hamiltonian Eq. (3), it also contains four electronic operators. In the definition of $\Lambda^{lmno}_{\mathbf{q}_\parallel,\mathbf{k}'}$ we have already integrated over $\mathbf{q}_\perp$ (the phonon wave vector perpendicular to the QW), in order to obtain a potential which can be directly compared to $V^{lmno}_{\mathbf{p}}$. $\Lambda^{lmno}_{\mathbf{q}_\parallel,\mathbf{k}'}$ can be negative and thus attractive for a certain range of parameters, see Fig. 2. In a strong coupling regime, this p-p attraction is responsible for bipolaron formation, i.e., a bound pair of polarons within a single band, despite Coulomb repulsion [5,15]. Here, however, we focus on the effects of polaron formation and interaction on the ISB repellon in a weak e-ph coupling regime, such as in GaAs. As the coupling mechanism occurs in momentum space, the nature of p-p attraction corresponds more to dynamical effects like Cooper pairs [16]. The relevant p-p coupling matrix elements for the polaronic repellon are $V^{2121}_{\mathbf{p}}$ and $\Lambda^{1221}_{\mathbf{q}_\parallel,\mathbf{k}'}$, shown in Fig. 2. Even for weak coupling, the attraction through $\Lambda^{lmno}_{\mathbf{q}_\parallel,\mathbf{k}'}$ (dotted line) can exceed the repulsion of $V^{2121}_{\mathbf{p}}$ (dashed line) for certain values of $\mathbf{q}_\parallel$, $\mathbf{k}$. For small values of $\mathbf{p}$, however, the direct Coulomb interaction diverges and is clearly the dominant component. Beyond a certain value of $\mathbf{q}_\parallel$ (where $E^{mn-}_{\mathbf{k}'+\mathbf{q}_\parallel,\mathbf{k}'} = 0$), the p-p interaction becomes repulsive. For nonvanishing values of $\mathbf{k}'$, this point shifts towards lower values of $\mathbf{q}_\parallel$, if $\mathbf{k}'$ has a component parallel to $\mathbf{q}_\parallel$, and in the other direction otherwise. From a direct comparison of the potentials as a function of $\mathbf{q}_\parallel$ or $\mathbf{p}$, one would conclude that the Coulomb interaction is by far the more important compo-

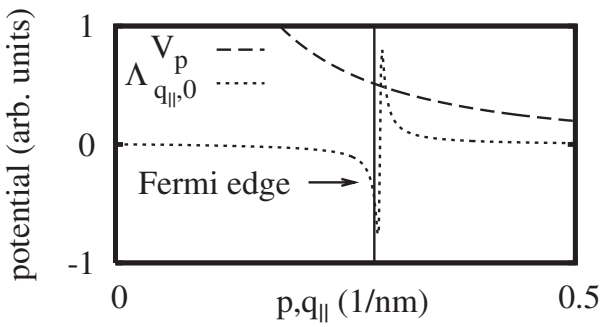

FIG. 2. Comparison of $V^{2121}_{\mathbf{p}}$ and $\Lambda^{1221}_{\mathbf{q}_\parallel,0}$, for a 10 nm wide GaAs QW. Fermi edge—for a carrier density of 1.2×10^{12} cm^{-2}.

nent. Yet, the formation of the repellon resonance occurs at the Fermi edge, thus especially Coulomb coupling matrix elements with wave vectors around the Fermi edge are essential for the repellon formation. If the Fermi edge is located at the point where $\Lambda^{lmno}_{\mathbf{q}_\parallel,0}$ reaches its minimum, [cf. Fig. 2], the shift of oscillator strength from low momentum states to the Fermi edge due to Coulomb repulsion is completely counterbalanced by the p-p attraction. In the case of states with $\mathbf{k}' \gg 0$, this interplay of effects is somewhat more complex, but the overall effect is similar. Note that the approach used here is similar to the Lee-Low-Pines approximation in a variational technique [17].

The experimentally controllable parameters are the temperature and the carrier density. Therefore, we propose to tune the Fermi edge through doping in an experiment until we reach this level of ISB p-p attraction; cf. Fig, 2. For lower carrier densities, only small values of $\mathbf{q}_\parallel$ matter, and we expect no significant contribution of the p-p attraction. Otherwise, for higher doping densities, the repulsive part of $\Lambda^{1221}_{\mathbf{q}_\parallel,\mathbf{k}}$ becomes relevant, i.e., the attractive and repulsive contributions can cancel each other and we get no overall effect; cf. Fig. 5. At higher temperatures, the repellon formation is less pronounced due to a softening of the Fermi edge. We hence expect the same behavior for the p-p attraction.

(iii)*Equations of motion for* e-ph *interaction.*—The Hamiltonian in Eq. (8) cannot reproduce the full set of equations of motion of the e-ph interaction, since the dephasing part [δ-function contribution, Eq. (6)] cannot be incorporated. In order to obtain the full equations of motion, we consider the equation of motion method [12] to obtain an equation for $f^{12}_{\mathbf{k}}$, which determines the optical spectra. In the second Born-Markov approximation we get [7]

$$\dot{f}^{\,12}_{\mathbf{k}}|^{e-}_{p} = -\sum_{\mathbf{q}} (\pi\Gamma^{\delta}_{1} + i\Gamma^{\mathcal{P}}_{1}) f^{12}_{\mathbf{k}} + (\pi\Gamma^{\delta}_{2} + i\Gamma^{\mathcal{P}}_{2}) f^{12}_{\mathbf{k}+\mathbf{q}_\parallel}. \quad (9)$$

An explicit expression for the $\Gamma^{\delta}_{i} = \Gamma^{\delta}_{i}(\mathbf{k},\mathbf{q})$ terms can be found in Ref. [7] [$\Gamma^{\mathcal{P}}_{i} = \Gamma^{\mathcal{P}}_{i}(\mathbf{k},\mathbf{q})$ is obtained by replacing $\delta(x)$ with $\mathcal{P}(1/x)$]. At low temperatures, this equation can be found similarly to the procedure in (ii).

The real part of the right-hand side of Eq. (9) contributes to the dephasing. The term containing $\Gamma^{\mathcal{P}}_{1}(\mathbf{k},\mathbf{q})$ is responsible for the polaron shift. For the e-ph coupling strength of GaAs this is, however, only a small shift of the ISB resonance of less than 1 meV. The last term, containing $\Gamma^{\mathcal{P}}_{2}(\mathbf{k},\mathbf{q})$, is the most interesting contribution, as it contains the polaronic contribution to the Coulomb induced repellon, which can also be seen from the formal analogy to Eq. (4).

(iv)*Numerical results.*—For the numerical evaluation, standard GaAs parameters [18] are used. The optical absorption is calculated at experimentally relevant temperatures $T = 4$, 77, and 300 K and a carrier density of 1.2×10^{12} cm^{-2}. Before we consider the full theory, we reduce the discussion to the e-ph interaction only. This helps to understand the effects of the p-p attraction on the optical spectra. Without the Coulomb repulsion the nature of the p-p attraction yields a bound state, arising through the fact that both polarons only see the positively charged background of the other polaron, but not the other's negative charge. Figure 3 shows the absorption spectra at different temperatures with the e-ph interaction reduced to dephasing (only Γ^{δ}_{i}) and including polaron effects (also $\Gamma^{\mathcal{P}}_{i}$), i.e., including the p-p attraction. At 300 K, [Fig. 3(a)] only a small polaron shift occurs, since the dephasing contributions (Γ^{δ}_{i}) are dominant, which contribute to a broadening of the ISB resonances [7]. However, pronounced differences with and without p-p attraction arise already at 77 K [Fig. 3(b)]. The sharpening of the line shape corresponds to the formation of a bound p-p state (which of course in this purity only exits without Coulomb repulsion). At 4 K [Fig. 3(c)], this effect is more pronounced. This shows that at low temperatures a reduction of the e-ph interaction to dephasing only may not be justified and explains the differences in line width observed between a Markovian reduced to dephasing and non-Markovian treatment of the e-ph interaction [19].

We now include the Coulomb e-e interaction, since both contributions (e-e, e-ph) occur on the same level of approximation, by taking into account Coulomb Hartree-Fock and scattering effects in the second order Born-Markov approximation [7,8]. For the considered carrier densities, screening effects are relevant [20], and we therefore include dynamical screening for the e-e and e-ph interaction [13,21]. Figure 4 shows the absorption spectra including both the Coulomb interaction and the e-ph interaction, with and without p-p attraction. Compared to Fig. 3, due to the Coulomb e-e exchange interaction, the spectra are shifted to higher energies. Without the p-p attraction, primarily seen at 4 K [Fig. 4(c)], the line shape is dominated by the sharp repellon resonance at the Fermi edge (dashed line) [6]. This effect is counterbalanced by the p-p attraction (solid line), i.e., the formation of a polaronic repellon which leads to a back shift of the oscillator strength towards the Γ point. As a result, the overall line width of the ISB transition changes (solid line). At 4 K, the FWHM increases by a factor of 5 through the

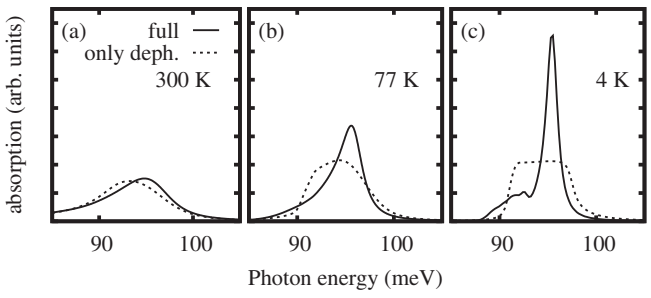

FIG. 3. Absorption spectra with e-ph interaction in a GaAs QW with a carrier density of 1.2×10^{12} cm^{-2}, considering the full dynamics (solid) and with dephasing only (dashed) at a temperature of (a) 300, (b) 77, and (c) 4 K.

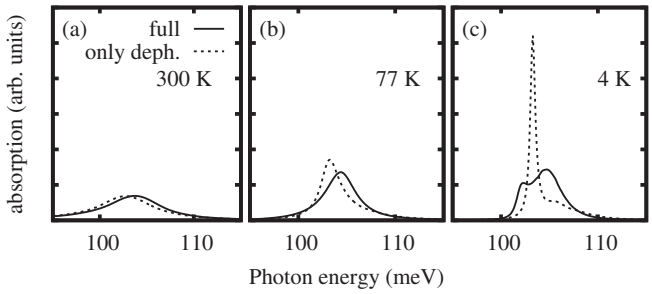

FIG. 4. Absorption spectra with e-ph and e-e interaction in a GaAs QW with a carrier density of 1.2×10^{12} cm^{-2}. Considering the full dynamics(solid), with dephasing for the phonons only (dashed). (a) 300, (b) 77, and (c) 4 K.

p-p attraction. For a non-Markovian treatment of the e-ph interaction, this increase of line width is slightly larger. At 77 K, these differences are already of minor importance and at 300 K [Fig. 4(a)] the absorption spectra have become identical.

The broadening of the line width at low temperatures essentially depends on the position of the Fermi edge, i.e., on the carrier density, since the significant p-p attraction is localized in a small $\mathbf{k}$ range. This is shown in Fig. 5. There are effectively no changes in the line shape or width for a carrier density of 0.6×10^{12} cm^{-2}. At 1.8×10^{12} cm^{-2}, we only find minor differences and almost no line broadening. In comparison to Fig. 4(c) this illustrates the density dependence of the effect. The observed discrepancy of line width, of a GaAs sample with a carrier density of 0.98×10^{12} cm^{-2}, in Ref. [8] between the calculations and the experiments at low temperatures might be explained by the polaronic repellon. Note, however, that in this sample interface roughness (not considered here) plays an important role.

In conclusion, we have shown that the interaction of electrons with LO phonons introduces an attractive p-p interaction in ISB systems. We have thereby shown that a reduction of the e-ph interaction to dephasing only is not valid in a low temperature regime. Furthermore, we showed, that this effect strongly depends on the doping density of the sample. Including the Coulomb interaction we found the formation a polaronic repellon, i.e., a repellon

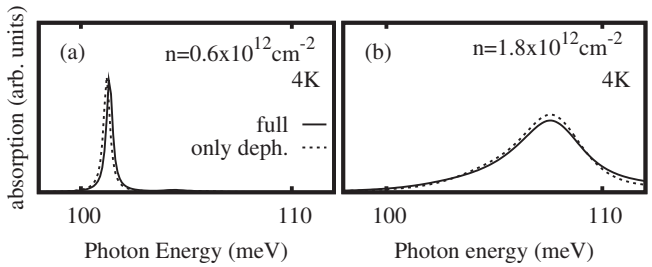

FIG. 5. Absorption spectra with e-ph and e-e interaction in a GaAs QW at 4 K with a carrier density of (a) 0.6×10^{12} cm^{-2} and (b) 1.8×10^{12} cm^{-2}.

resonance, which is modified by the p-p attraction. In particular, at 4 K and for a carrier density around 1.2×10^{12} cm^{-2}, this interplay of effects leads to a line broadening, not predicted by earlier descriptions. Since the Fermi edge can be tuned, this broadening of the line width should be observable in experiments. Polaronic repellons occur already in weak coupling systems such as GaAs due to the Fermi edge character of repellons.

We acknowledge financial support by the Deutsche Forschungsgemeinschaft and thank Inès Waldmüller (Sandia National Laboratories), Julia Unterhinninghofen, Marten Richter, Carsten Weber (TU Berlin), Michael Woerner, and Klaus Reimann (Max Born Insitut Berlin) for helpful discussions.

*Electronic address: butscher@itp.physik.tu-berlin.de

[1] T. Elsaesser and M. Woerner, Phys. Rep. **321**, 253 (1999).
[2] M. F. Pereira and H. Wenzel, Phys. Rev. B **70**, 205331 (2004).
[3] R. Iotti and F. Rossi, Semicond. Sci. Technol. **19**, S323 (2004).
[4] B. Nottelmann, V. Axt, and T. Kuhn, Physica (Amsterdam) **B272**, 234 (1999).
[5] J. T. Devreese, *Encyclopedia of Applied Physics* (VCH, Weinheim, 1996), Vol. 14, p. 383.
[6] D. E. Nikonov, A. Imamoglu, L. V. Butov, and H. Schmidt, Phys. Rev. Lett. **79**, 4633 (1997).
[7] I. Waldmüller, J. Förstner, S. C. Lee, A. Knorr, M. Woerner, K. Reimann, R. A. Kaindl, T. Elsaesser, R. Hey, and K. H. Ploog, Phys. Rev. B **69**, 205307 (2004).
[8] J. Li and C. Z. Ning, Phys. Rev. B **70**, 125309 (2004).
[9] F. Banit, S. C. Lee, A. Knorr, and A. Wacker, Appl. Phys. Lett. **86**, 041108 (2005).
[10] T. Ando, Z. Phys. B **24**, 33 (1976).
[11] T. Kuhn, in *Theory of Transport Properties of Semiconductor Nanostructures*, edited by E. Schöll (Chapman and Hall, London, 1998), Chap. 6, p. 173.
[12] I. Waldmüller, J. Förstner, and A. Knorr, *Nonequilibrium Physics at Short Time Scales* (Springer, Berlin, 2004), p. 251.
[13] H. Haug and S. Koch, *Quantum Theory of the Optical and Electronic Properties of Semiconductors* (World Scientific, Singapore, 2004).
[14] M. Schubert and B. Wilhelmi, *Nonlinear Optics and Quantum Electronics* (John Wiley & Sons, New York, 1986).
[15] A. Alexandrov and N. Mott, Rep. Prog. Phys. **57**, 1197 (1994).
[16] S. Dzhumanov, A. A. Baratov, and S. Abboudy, Phys. Rev. B **54**, 13 121 (1996).
[17] T. Lee, F. Low, and D. Pines, Phys. Rev. **90**, 297 (1953).
[18] $m_1 = 0.071 \times m_0$, $m_2 = 0.087 \times m_0$, $\varepsilon_{\text{gap}}(\mathbf{k} = 0) = 98.54$ meV, $n_D = 1.2 \times 10^{12}$ cm^{-2}, width $L = 10$ nm.
[19] S. Butscher, J. Förstner, I. Waldmüller, and A. Knorr, Phys. Status Solidi B **241**, R49 (2004).
[20] X. G. Wu, F. M. Peeters, and J. T. Devreese, Phys. Status Solidi B **133**, 229 (1986).
[21] G. Mahan, *Many-Particle Physics* (Kluwer, New York, 2000), Chap. 7.3, 3rd ed.